Surface & Coatings Technology 425 (2021) 127694

Contents lists available at ScienceDirect

Surface & Coatings Technology

journal homepage: www.elsevier.com/locate/surfcoat

Conductive epoxy/carbon nanofiber coatings for scale control

Laura Edvardsen [a,*], Mathieu Grandcolas [b], Sigrid Lædre [a], Juan Yang [b], Torstein Lange [a], Ruben Bjørge [a], Kamila Gawel [a]

[a] SINTEF Industry, 7465 Trondheim, Norway
[b] SINTEF Industry, 0314, Oslo, Norway

ARTICLE INFO

Keywords:
Scale inhibition
Calcium carbonate
Carbon nanofiber
Anodic polarization
Epoxy coating

ABSTRACT

Calcium carbonate ($CaCO_3$) is one of the most widespread scaling minerals and has been a long-standing problem within many industrial sectors. Scaling of calcium carbonate on conductive surfaces can be prevented electrochemically by anodic polarization. Anodic polarization, however, cannot be applied directly to metal surfaces like e.g., steel that will suffer from corrosion when polarized anodically in an aqueous environment. Thus, in this paper it is proposed to apply a conductive coating to a metal surface to allow anodic polarization and inhibit surface scaling, without corrosion of the underlying metal surface taking place. To this end an epoxy/carbon nanofiber conductive coating was developed and deposited at steel surfaces. The coating showed good adhesion to the surface and the bulk and surface resistivities were in the order of 52.80 kΩcm and 31.87 kΩ/cm^2, respectively. The anti-scaling performance of the coating without- and under anodic polarization was tested upon exposure to 1.5 wt% $CaCl_2$ solution being in contact with CO_2. The coating has been tested at several different potentials to find optimal conditions for scale inhibition. Potentials above +3 V_{OCP} caused a degradation of the coating due to oxygen evolution at the anode, as well as evolution of chlorine gas. At +1.5 and + 2 V_{OCP} the coating remained intact and the precipitation of $CaCO_3$ was limited. On the other hand, cathodic polarization of the coating surface enhanced scaling and no coating degradation was observed at cathodic polarization even at potentials as high as −5 V_{OCP}. The coating has thus proven a good solution to control surface scale deposition. Both anodic scale inhibition and cathodic scale acceleration have been achieved at the coating surfaces.

1. Introduction

Calcium carbonate ($CaCO_3$) is one of the most common scaling minerals, and can cause economic and technical problems within many industrial sectors [1]. Undesirable scale formation can clog pipelines or wells in the oil and gas industry, limit the power produced in cooling towers in nuclear power plants and is a major obstacle in geothermal energy facilities [1–3]. Precipitation of $CaCO_3$ scales in water systems can promote pathogenic microbial proliferation (e.g., *Legionella*) [4], which can lead to diseases. Scaling of filtration membranes by $CaCO_3$ is also a frequent challenge in wastewater reclamation and desalination facilities [5,6].

There are many factors that affect the formation of $CaCO_3$ scales, including pH, temperature and oversaturation level [7]. The solubility of $CaCO_3$ is dependent on the pH and the precipitation of $CaCO_3$ increase with increasing pH [7]. Precipitation of $CaCO_3$ occurs spontaneously at alkaline conditions, while an acidic environment prevents precipitation and supports dissolution [8]. The effect of temperature on $CaCO_3$ precipitation is not as significant as the effect of pH, but increasing temperature leads to an increase of the precipitation rate [7]. The precipitation rate of $CaCO_3$ also increases with increased concentration of calcium in the solution [7,9].

The most common scale inhibition strategies include chemical, physical and biological treatment methods [7]. One of the most commonly used scaling control method is chemical inhibition, where a chemical that retards precipitation of $CaCO_3$ is added to potentially scaling waters (e.g., Polyacrylate, Phosphonic acids, PBTCA). Chemical inhibition is popular in oil and gas industry, but such inhibitors may not be acceptable in water supply infrastructure. Therefore, alternative inhibition methods have been developed to reduce or fully prevent scale formation. Ultrasonic cleaning is an established technology for removal of biological fouling and can be used as a scale inhibition method by acoustic cavitation-generated erosion of scale deposits [10]. Electromagnetic water treatment is an alternative solution for scale control, but

* Corresponding author.
E-mail address: laura.edvardsen@sintef.no (L. Edvardsen).

https://doi.org/10.1016/j.surfcoat.2021.127694
Received 21 June 2021; Received in revised form 27 August 2021; Accepted 5 September 2021
Available online 10 September 2021

the literature data describing efficiency of this method are not consistent [11–13] and the electromagnetic scale inhibition mechanisms are not entirely understood [14,15]. Surface modification methods and coatings are a mitigation method where the molecular interactions between the surface and deposits are modified to inhibit adhesion of scales [16,17]. Surface treatment methods aim on enhancing the scale removal during hydrodynamic or mechanical cleaning. An ecological and efficient method to inhibit scale formation is electrochemically enhanced deposition [4] that relies on decreasing the content of scaling ions in the solution by precipitating them on an electrode (cathode) surface. The precipitation is facilitated due to local increase of pH at the cathode due to reduction of hydrogen and generation of hydroxide ions [18]. In contrast to the cathode, the local pH at anode is acidic due to the oxidation reactions leading to the formation of hydrogen ions [4,9,19].

Since the solubility of $CaCO_3$ increases with decreasing pH, anodic polarization of a surface can be utilized to decrease the local pH and thus prevent calcium carbonate scaling. It has been previously shown that cathodic polarization accelerates the deposition of $CaCO_3$ on a graphite surfaces, while an anodic polarization inhibited the deposition [9]. The anodic polarization as a method to prevent scaling is however limited to materials that will not undergo corrosion when anodically polarized. Steel is one of the most widely used materials in the world due to its high durability, strength, low cost and thermal conductivity [20]. However, when polarized anodically the corrosion rate increases. Replacing steel with a noncorrosive material to take advantage of anodic polarization against scaling is often not a viable approach due to the specific requirements on mechanical properties of construction elements. What could be a possible approach is to use a noncorrosive conductive coating as a barrier between the steel surface and a solution containing scaling minerals. This would allow for anodic polarization, and hence inhibition of deposition of pH sensitive scales, without sacrificing the steel.

The method of modifying non-conductive polymer matrix by incorporating conductive nanofillers has attracted a lot of attention in the past few years and carbon nanomaterials are of particular interest as conductive fillers. Especially, carbon nanofibers (CNF) represent, with a relatively mature manufacturing process, a cost-effective and commercially available solution with good electrical, thermal, and mechanical properties. Cardoso et al. prepared a CNF in epoxy composite by a simple dispersion method and reported conductivity values up to 10^{-2} mS/cm for 3 wt% CNF [21]. A few other authors reported CNF dispersion methods (e.g., ultrasonication and mechanical mixing) in epoxy resins and their relation to microstructure and electrical properties [22–29].

The main objective in this work was to investigate the utility of a nanocomposite material made of epoxy resin and carbon nanofibers as a conductive coating aiming on preventing $CaCO_3$ scaling upon anodic polarization. CNF composite with polyamide used as a reversed osmosis membrane has previously been shown to retard calcium carbonate and calcium sulphate scaling upon application of anodic polarization [30]. It has thus been hypothesized that conductive, CNF/polymer coating when deposited on steel surface can (i) prevent the steel surface from corrosion upon anodic polarization conditions and (ii) prevent surface from scale deposition at the same polarization conditions. To test this hypothesis, it was deposited epoxy/CNF coating on a stainless-steel surface and then tested for anti-scaling performance under different anodic polarization conditions (polarization potentials).

2. Materials and methods

2.1. Preparation of epoxy/CNF coatings

The as-received carbon nanofibers (CNFs, Pyrograf® III, Applied Sciences Inc.) were first mixed with the epoxy resin (Araldite® model 2020 from Hunstman, part A) with a wooden spatula until all powder was incorporated. The hardener (part B) was then added to the mixture to obtain a resin/hardener ratio of 10:3 (*w*/w). The CNF content in the resulting material was 3 wt%. To further disperse the CNFs in the epoxy, the blend was mixed using a planetary mixer (Thinky ARE-310) for 5 min at 2000 rpm and defoamed for 40 s at 1500 rpm. Stainless-steel disks (Ø40 mm SS316, previously cleaned with acetone and ethanol) were coated with the epoxy/CNF mixture using a simple paint brush. All samples were cured at room temperature overnight and then heat treated at 80 °C for 1 h.

2.2. Water contact angle measurements

The water contact angle on coated and uncoated surfaces was measured using a OSSILA goniometer (10 μL drop using distilled water for each measurement). The contact angle was measured on a bare SS316 sample, an epoxy/CNF coated sample and an epoxy coated reference sample without CNF. The average contact angle was calculated based on the five measurements for each sample.

2.3. Electrical resistance measurements

A cylindrical epoxy/CNF sample with thickness and diameter of 11.3 and 24.6 mm, respectively, was used to measure the volume resistivity. The surface resistivity was measured for an epoxy/CNF coated SS316 sample. The electrical resistance was measured using a Fluke 123 ScopeMeter (20 MHz). The electrical contacts were made using Epo-Tek® H21D (Epoxy Technology) epoxy/silver composite dedicated for electronic applications. The resistance measured for the hardened epoxy/silver was in the order of 1–3 Ω.

2.4. Experimental setup for testing anti scaling properties of epoxy/CNF coatings

A three-electrode system and a Gamry Reference 600 potentiostat was used for all the electrochemical tests presented in this paper. The working electrode (WE) was a coated SS316 disk placed inside a setup (electrochemical short-pipe) where only one side of the sample was exposed to the electrolyte, see Fig. 1.

A graphite rod was used as counter electrode (CE) (also visible in Fig. 1), while an Ag/AgCl reference electrode (RE) was connected to the system via a salt bridge. Cathodic and anodic potentials were applied to different samples in order to increase and reduce precipitation of $CaCO_3$, respectively. All potentials were set vs. OCP (Open Circuit Potential), while the measured potentials are given vs. Ag/AgCl. The electrolyte (1800 mL), or scaling solution, contained 1.5 wt% $CaCl_2$ (Merck KGaA) and had a pH of 12, adjusted by adding sodium hydroxide (NaOH, Merck KGaA) right before start-up of the experiment. Scaling was induced by introducing gaseous CO_2 to the solution at a gas rate of 5.6 mL/min. The potential between WE and CE was applied simultaneously as CO_2 was introduced to the system. Linear Sweep Voltammetry (LSV) experiments were conducted by sweeping the potential linearly between +0.8 and + 4 V_{OCP} at a scan rate of 1 mV/s while measuring the current at the WE.

Potentiostatic experiments with coated steel as an anode were conducted at +1.5, +2, +3 and + 5 V_{OCP}, and then as a cathode at −2, −3 and − 5 V_{OCP}. A coated steel disk was also exposed to the scaling solution without any applied potential to act as a reference sample. All of these experiments were performed in a fume hood at room temperature (23 °C ± 2 °C) and atmospheric pressure with a duration of 45 min. After the experiments, the samples were immersed in deionized water for 2 s to remove the excess of ions. This was done to prevent crystallization of the remaining salts during the following drying process. To investigate how the coating endured longer polarization periods, additional experiments were carried out where samples were exposed to +5 V_{OCP} and + 1.5 V_{OCP} for 6 h.

2.5. Scanning electron microscopy (SEM)

Scanning electron microscopy (SEM) imaging of the sample surface before and after exposure to the scaling solution was performed using a

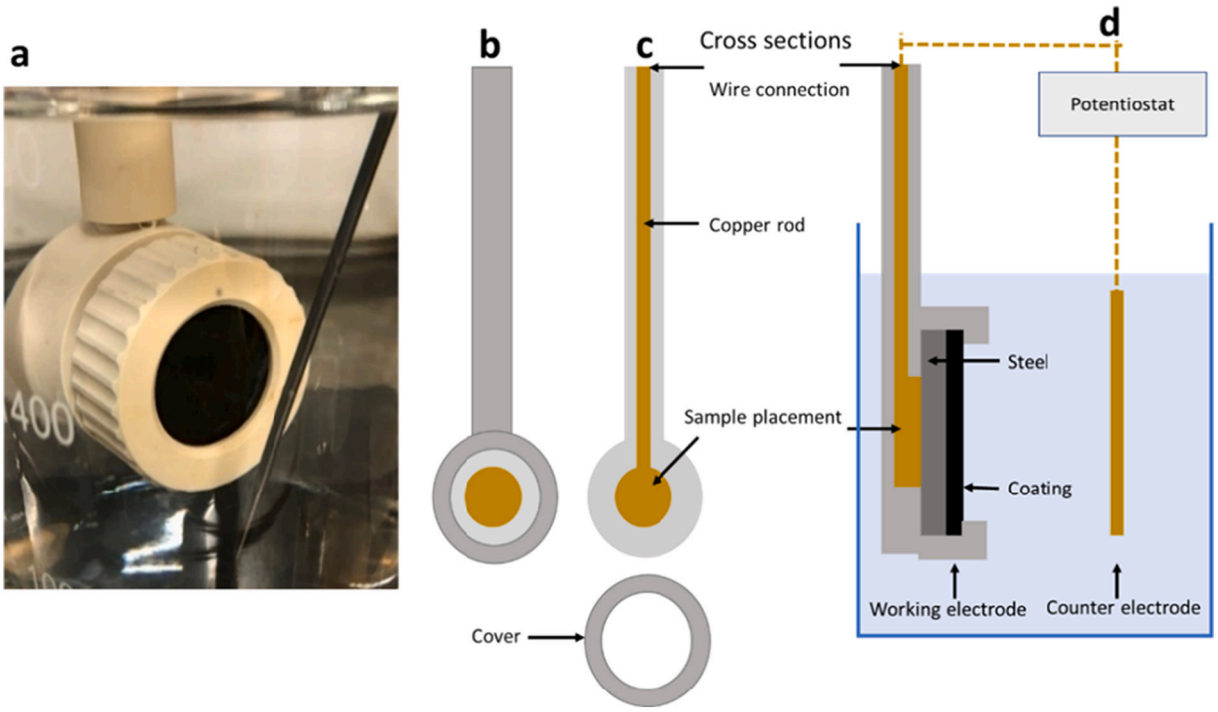

Fig. 1. Photography of the working electrode (containing a SS316 disk coated with epoxy/CNF) (a) and sketch of the working electrode setup: (b) top view of the sample holder, (c) cross-section of the working electrode design with cover used to control the exposed area of the sample and (d) sketch showing side view of the working electrode with steel/coating sample placed in the holder being a part of the whole exposure setup including working electrode, counter electrode and potentiostat. Not included is the Ag/AgCl reference electrode.

Hitachi S-3400 N operated at 15 kV. The images were acquired in back-scattered electron mode.

2.6. X-ray micro-computed tomography (μ-CT)

In order to validate homogeneity of the resulting epoxy/CNF composite material, X-ray micro-computed tomography (μ-CT) was performed using an industrial CT scanner (XT H 225 ST). The operational voltage and current were 165 kV and 60 μA, respectively. The raw CT data was later reconstructed into cross sectional slices.

3. Results and discussions

3.1. Morphology

The thickness of the epoxy/CNF coating deposited on stainless steel disks ranged between 0.8 and 1 mm. The coating was relatively homogeneous as indicated by the X-ray tomography image shown in Fig. 2. The presence of relatively well spread dark spots with sizes smaller than 0.25 mm suggests that the inhomogeneities are constituted of lower density material (compared to the density of the epoxy resin matrix) that could be either CNF aggregates, air bubbles, or both. However, the larger spots are associated with air bubbles.

3.2. Resistivity

The epoxy/CNF material bulk resistivity was estimated to be 52.80 kΩcm and surface resistivity was 31.87 kΩ/cm^2. The obtained resistivity values are higher than those reported elsewhere [31] for similar content of CNFs but both epoxy resin as well as mixing procedure and also carbon nanofiber type were different in the work reported herein compared to results reported by Czyzewski et al. [31].

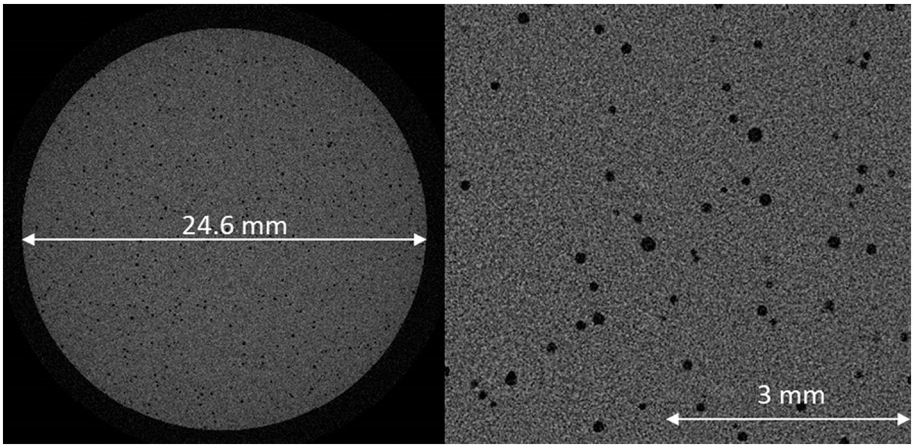

Fig. 2. X-ray tomography cross-section through the epoxy/CNF coating material (left) and an enlarged area from the scan (right).

3.3. Wettability

The water contact angle of pure epoxy was measured to be around 61°, while the contact angle measured on epoxy/CNF coating was 72°. Carbon nanomaterials are hydrophobic and as such they are expected to contribute to the decreased water wetting capability (increased water contact angle) [32]; nevertheless, the surface wetting of epoxy/CNF is still high and the surface is considered hydrophilic since the contact angle is less than 90° [33]. The contact angle of a bare SS316 sample was 83°.

3.4. Electrochemical surface activity upon polarization

Fig. 3 displays the results from the linear sweep voltammetry experiments where the voltage was swept from +0.8 to +4 V_{OCP}. The area of the curve where the current density was lowest, is where the reaction on the electrode surface changes from cathodic to anodic (open circuit potential). In order to obtain comparable results both samples were left for approximately 5 min in the electrolyte before polarization to avoid any unwanted reactions prior to polarization. Stabilization of OCP on bare stainless steel can take a long time [34], and this was most likely the reason why the cathodic part of the curve is missing. However, corrosion potential (E_{corr}) can be found from the anodic curve in Fig. 3. For the bare steel sample, E_{corr} is approximately +0.6 $V_{Ag/AgCl}$ while the coated surface shows open circuit potential of approximately +1.7 $V_{Ag/AgCl}$. As the coating is non-metallic, and no traces of corrosion were found on the metal substrate, it is likely that the currents produced on the coated sample surface were due to other electrochemical reactions than corrosion. The increase in current density could be associated with electrolytic processes taking place on the surface of carbon nanofibers and/or be associated with coating degradation. Water splitting is one reaction which can take place on a polarized surface. One part of water splitting is the production of oxygen gas (OER) at the anode. This reaction is known to be kinetically limited, particularly in alkaline solutions [35]. The oxygen evolution potential depends on both electrode surface and electrolyte, where some surfaces are more catalytic towards oxygen evolution than others. Favaro et al. [36] investigated the oxygen evolution reaction on platinum surfaces in pH 12 KOH solutions, and their cyclic voltammetry test showed the OER to take place at 0.9 $V_{Ag/AgCl}$. Due to the presence of $CaCl_2$ in our electrolyte solution, chloride ions migrate towards the anode and are oxidized to chlorine gas through the following reaction.

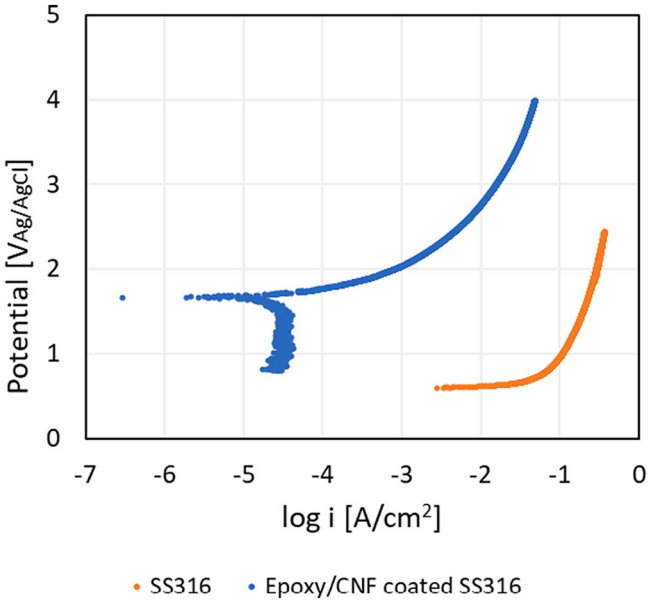

Fig. 3. Plot of potential against log i (i = current density = current/surface area) during a sweep from 0.8–4 V_{OCP} at a sweep rate of 1 mV/s. The potential of the working electrode is versus the Ag/AgCl reference electrode and is controlled by the linear sweep voltammetry software of the potentiostat. The blue data points refer to epoxy/CNF coated SS316 as working electrode, and the orange data point to the non-coated SS316.

$$2Cl^- \rightarrow Cl_2 + 2e^- \quad (1)$$

The evolution of chlorine gas is known to attack graphite composites when polarized [37]. It is thus likely that the current increase seen in Fig. 3 is due to both OER and production of chlorine gas.

After the linear sweep voltammetry experiments (up to +4 V_{OCP}), no $CaCO_3$ precipitation was seen on the epoxy/CNF coated sample surface. The anti-scaling performance of the coating under polarization was tested in more detail through potentiostatic polarization as described in Section 3.5.

3.5. Performance of the coating in scale inhibition and acceleration

Fig. 4 shows SEM images which compare the surfaces of epoxy/CNF coating after polarization at +1.5, +2 V and − 2 V_{OCP} for 45 min in the scaling solution. At the end of the experiment the surface of the reference sample was covered with white precipitate. The amount of precipitate was significantly higher when the surface was cathodically polarized. On the other hand, anodic polarization led to significantly reduced scaling even at polarization potentials as low as +1.5 V_{OCP}. The increase of the anodic polarization potential to +2 V_{OCP} resulted in further reduction of the amount of the precipitate present at the surface.

The scaling potential of the 1.5 wt% $CaCl_2$ solution in contact with CO_2 is high, thus precipitation of the calcium carbonate minerals is expected both in the solution bulk but also on the surfaces exposed to this solution [9]. Due to high initial pH (value of 12), the carbonic acid formed in the CO_2 saturated solution dissociates almost completely to form hydrogen and carbonate ions. The carbonate ions react with calcium ions and form calcium carbonate precipitate, which leads to a scale build-up. Due to the injection of CO_2, the pH of the electrolyte will decrease with time. In similar experiments, Edvardsen et al. [9], the pH close to the anode decreased faster than the pH measured in the bulk solution and close to the cathode. This was due to the electrochemical processes at the electrodes.

Calcium carbonate precipitation is pH sensitive [7]. It undergoes at high pH while calcium carbonate dissolution is promoted at low pH values. It has been previously shown that polarization of conductive surfaces may lead to local pH changes close to electrodes [4,19]. This is the case especially when the polarization potential is above water splitting potential. It is expected that the local pH close to anode is acidic while close to cathode alkaline due to the following reactions taking place on cathode and anode, respectively.

$$2H_2O + 2e^- \rightarrow H_2 + 2OH^- \quad (2)$$

$$2H_2O \rightarrow O_2 + 4H^+ + 4e^- \quad (3)$$

The increased pH value of the solution near the cathode surface promotes the formation and adhesion of calcium carbonate crystals on cathode surface, while the acidic solution near the anode inhibits precipitation at the anode surface [19]. Similar reactions on conductive surfaces described previously in literature are expected to occur also on the surface of polarized epoxy/CNF composites or more specifically on the surface of carbon fibres in contact with electrolyte. Thus, the above-described mechanisms explain how polarization of epoxy/CNF coating can be utilized to control carbonate scale deposition on epoxy/CNF coated steel surfaces. The coating accelerates calcium carbonate deposition upon cathodic polarization while it inhibits surface deposition of carbonate scale at anodic polarization and protects the underlying metal surface from corrosion. Fig. 5 depicts high magnification SEM images of different precipitation states (anode and cathode) obtained on the epoxy/CNF surfaces of two different samples. Although precipitates are

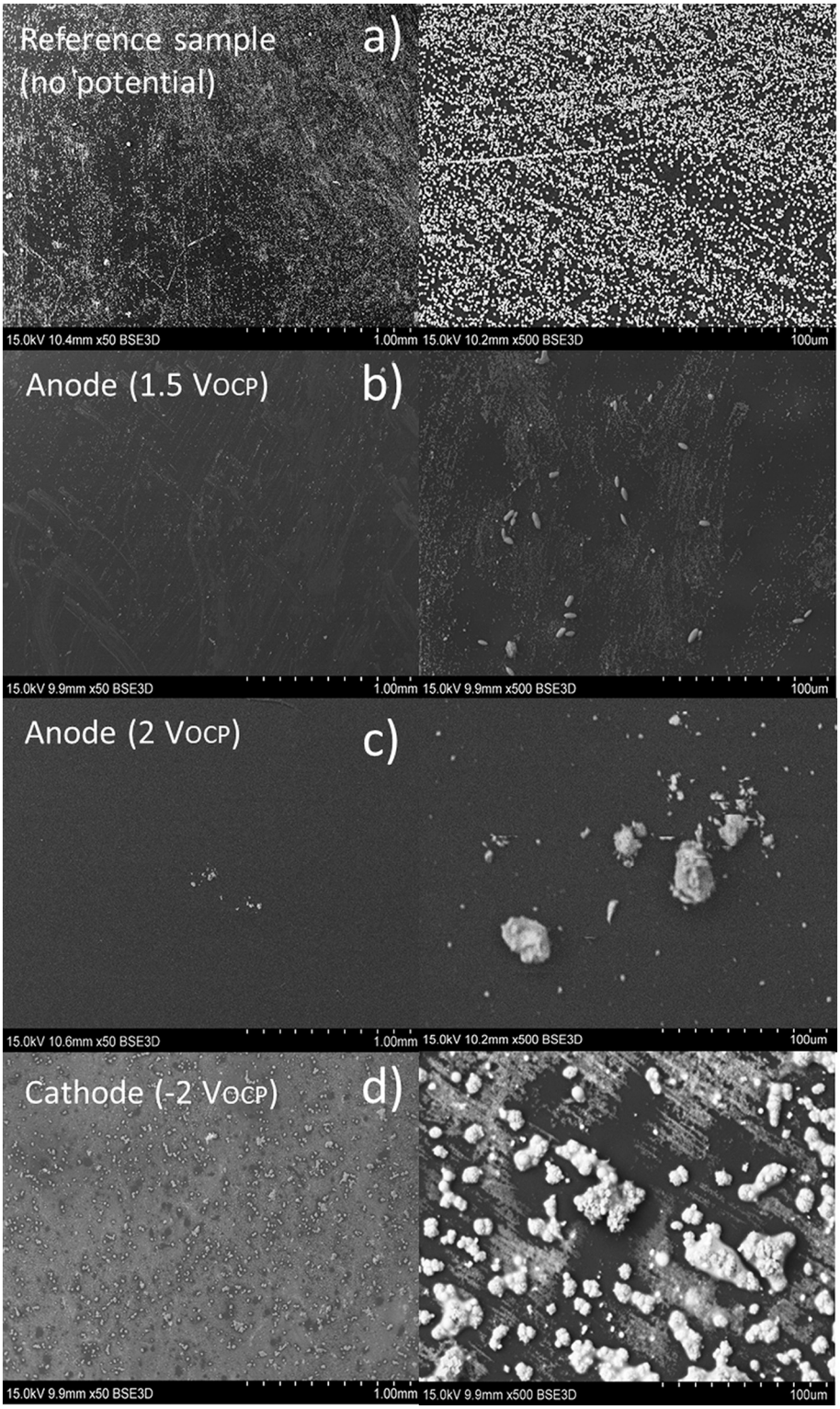

Fig. 4. SEM images presenting topography of (a) a reference sample (SS316 coated with epoxy/CNF without any polarization), and sample surfaces subjected to a potential of +1.5, +2 and − 2 V_{OCP} in the scaling solution for 45 min (b, c, d, respectively). The enlarged images (bar scale 100 μm) depict the largest features found in the 1 mm images and are thus not representative for the whole surface.

visible on both electrode surfaces, there are substantial differences in the amount and shape of precipitate. Anodic polarization caused the calcium carbonate crystals to aggregate into oval shapes of size 3–6 μm. For the sample polarized cathodically, larger amount of spherical shaped aggregations of $CaCO_3$ crystals with a diameter of 6–10 μm was the dominant morphology. A close-up of the crystals (Fig. 5d) showed that the spheres appeared to be spherical aggregates consisting of smaller rhombohedral units, which is known as spherulites [38].

3.6. Limitations: degradation at higher polarization potentials

While anodic polarization at +1.5 and + 2 V_{OCP} did not cause any

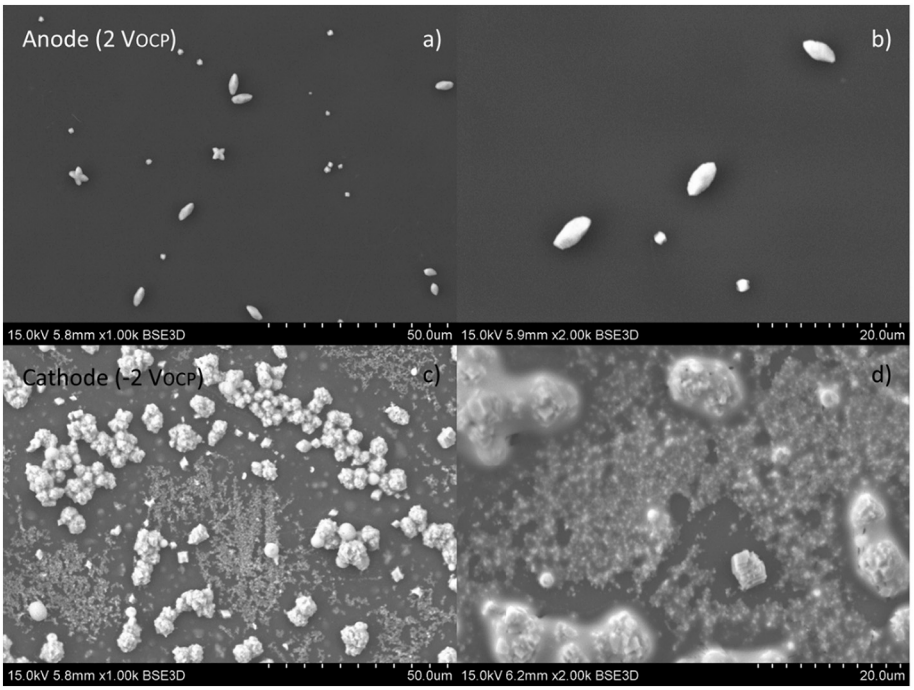

Fig. 5. SEM images presenting topography at high magnification of sample surfaces subjected to a potential of −2 V_{OCP} (a, b) and + 2 V_{OCP} (c, d). All samples were exposed to the scaling solution for 45 min. The surface areas investigated was selected in order to compare differences between precipitates at the anode and cathode.

degradation of the epoxy/CNF coating within the experiment timescale (45 min), the anodic polarization at +3 V_{OPC} and higher potentials resulted in the formation of blisters on the coating surfaces. The blisters were larger on the surface polarized at +5 V_{OCP} than on +3 V_{OCP} as shown by scanning electron microscopy imaging of the polarized surfaces presented in Fig. 6. This could have been caused by either electrochemical degradation of the coating or reactions due to the pH change induced by the high potential. As the epoxy resins are resistant to degradation within high pH ranges [39], it is likely that the degradation processes are associated with electrochemical reaction products, further reacting with either organic epoxy or CNF within the resin composite. It has been previously shown in the literature that epoxy/carbon composites can be susceptible to degradation under both cathodic and anodic polarization (e.g., Ofoegbu et al. [39]). The composite degradation is not due to electrochemical dissolution, like in the case of metals, but rather due to secondary chemical reactions involving electrochemically evolved species [39,40]. In the case of anodic polarization, adsorbed atomic oxygen, being an intermediate in the oxygen evolution reaction, have been linked to degradation [39]. According to Stafford et al. [37], the anodic degradation of epoxy/carbon composites is due to a combination of three effects: (i) chemical and electrochemical graphite oxidation; (ii) formation of cavitation due to the evolution of chlorine and oxygen gas, see reaction (1) and (3); (iii) as well as due to oxidation by active chlorine in acidic chloride solutions. It is thus most likely that the blisters observed on the epoxy/CNF surface polarized at +3 and + 5 V_{OCP} (see Fig. 6) are due to cavitation associated with chlorine and oxygen gas evolution. The detailed mechanism of polymer chain chemical degradation in the presence of chlorine and oxygen aqueous solutions has been described by Agrawal et al. [41]. Increasing the polarization potential leads to an increase in chlorine gas production and gas evolution at the anode, which results in more severe degradation of the epoxy/CNF coating.

Cathodic polarization at high polarization potentials (−3 and − 5 V_{OCP}) did not result in any visible surface degradation. According to Taylor et al. [42], cathodic polarization may lead to surface degradation, however the alkaline conditions hinder degradation [42]. On the other hand, the cathode epoxy/CNF surface was covered with a precipitate (most likely calcium carbonate). Cathodic polarization significantly enhanced scale precipitation at the surface (see Fig. 4, reference sample) due to pH rise mechanisms described above in reaction (2). The amount of the precipitate was greater for the sample polarized at −5 V_{OCP} than for the electrode polarized at −3 V_{OCP}. Also, the morphology of the crystallites deposited on the coating surface was different for the two polarization potentials. Larger crystals were observed for the polarization potential of −5 V_{OCP} compared to −3 V_{OCP}. This is in line with findings reported for the calcium carbonate deposition on the graphite surfaces reported elsewhere [9]. The deposited layers on the cathode surfaces were not uniform in contrast to the deposit on the reference sample (see Fig. 4). Within the precipitated layer there are visible circular shapes. The shapes are most likely imprints made by the forming and growing on the surface gas bubbles that protected the spot underneath from carbonate mineral deposition.

Fig. 7 presents photos of the steel sample coated with epoxy/CNF before and after polarization at +5 V_{OCP} for 45 min as well as a photo of the steel surface after the coating has been removed. The coating surface before the polarization is smooth, homogeneous, and glossy. After polarization, the roughness of the surface increases and the surface loses the glossy appearance. Simultaneously, no precipitate is observed on the polarized surface. The metal surface underneath the coating is intact and no evidence of corrosion is present. Fig. 7 also depicts a bare stainless-steel sample before and after anodic polarization. With no protective coating, the bare steel sample is subjected to severe corrosion. The macroscopic inspection indicates that: (i) anodic polarization of epoxy/CNF coatings offers protection against scaling; (ii) the coating protects the metal surface from corrosion, but (iii) the coating is susceptible to degradation at anodic polarization at high polarization potentials.

Fig. 8 depicts the current responses obtained for samples polarized both anodically and cathodically at various potentials for 45 min. At the anode, the surface current density increased in time from the moment the polarization is initiated and stabilized after around 10 min. The current on the anode increased with potential. At the cathode, the first increase in current density was observed within the first 3 min which was followed by a decrease. It is likely that the decrease at the cathode is associated with scale build-up on the surface and the reduction of

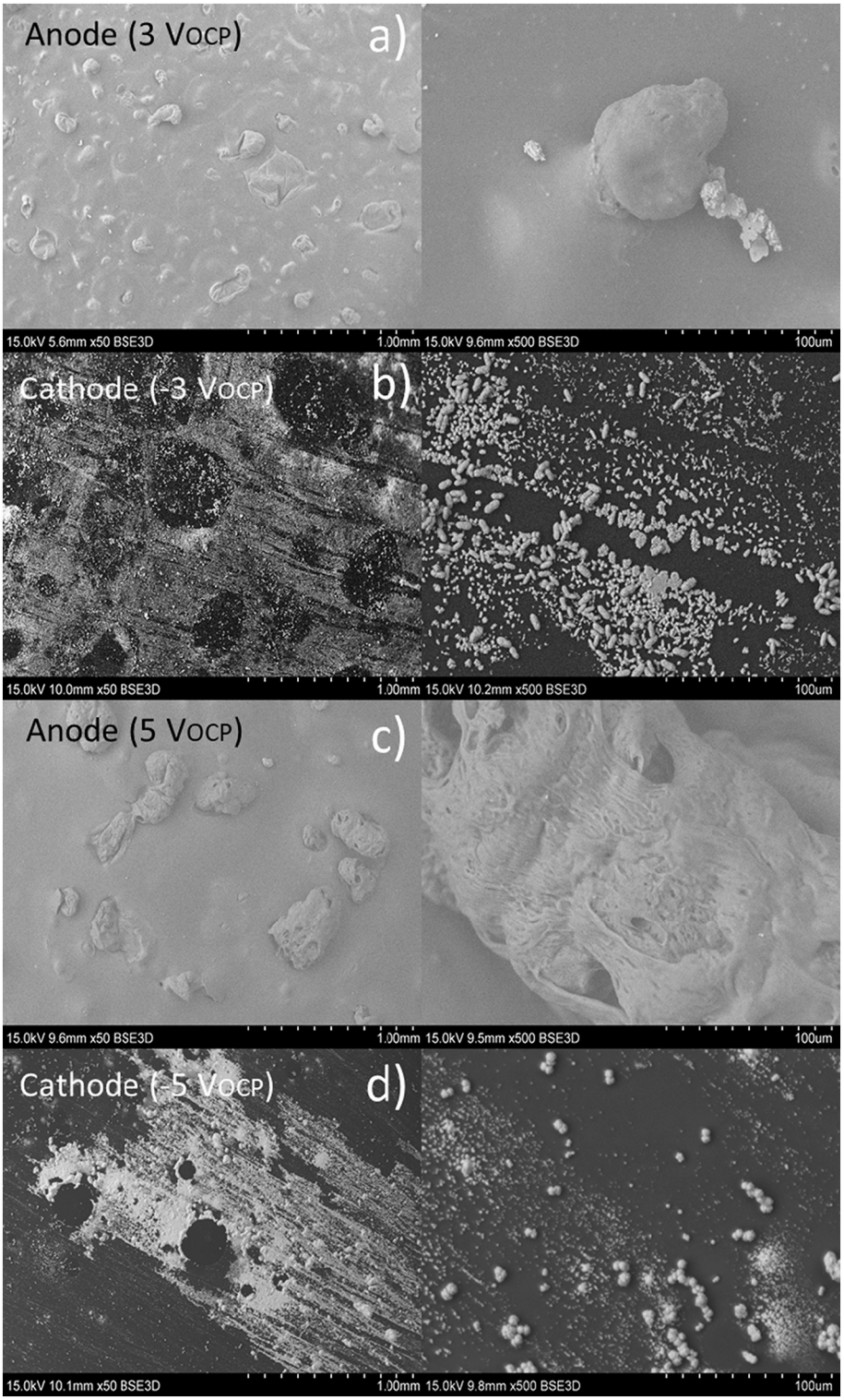

Fig. 6. SEM images presenting topography of sample surfaces subjected to a potential of +3, −3, +5 and − 5 V_{OCP} (a, b, c, d, respectively). All samples were exposed to the scaling solution for 45 min. The enlarged images (100 μm) depict the largest features found in the 1 mm image and are thus not representative for the whole surface.

effective conductive surface area due to precipitation of nonconductive mineral. As neither of the samples showed signs of substrate corrosion after anodic polarization, it is unlikely that the currents came from corrosion of underlying metal surface. At potentials above the water splitting potential (1.23 V [43], but also depending on overpotentials and how catalytic the coating is towards this reaction), oxygen evolution is to be expected. In addition, other electrochemical reactions, such as degradation of the coating and chlorine gas production could have contributed to the currents seen in Fig. 8.

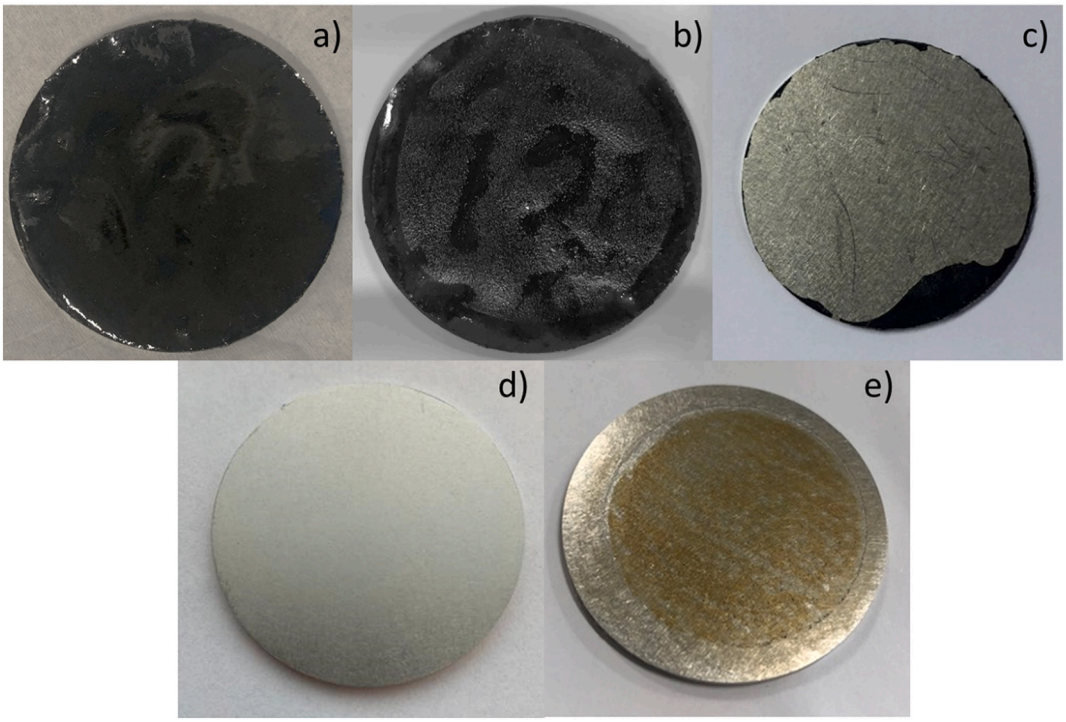

Fig. 7. Photography of SS316 samples coated with epoxy/CNF before (a) and after (b) anodic polarization at +5 V_{OCP} for 45 min, (c) the intact surface of stainless steel after the epoxy/CNF coating had been removed, and a stainless-steel sample without coating before (d) and after (e) anodic polarization at +5 V_{OCP} for 45 min.

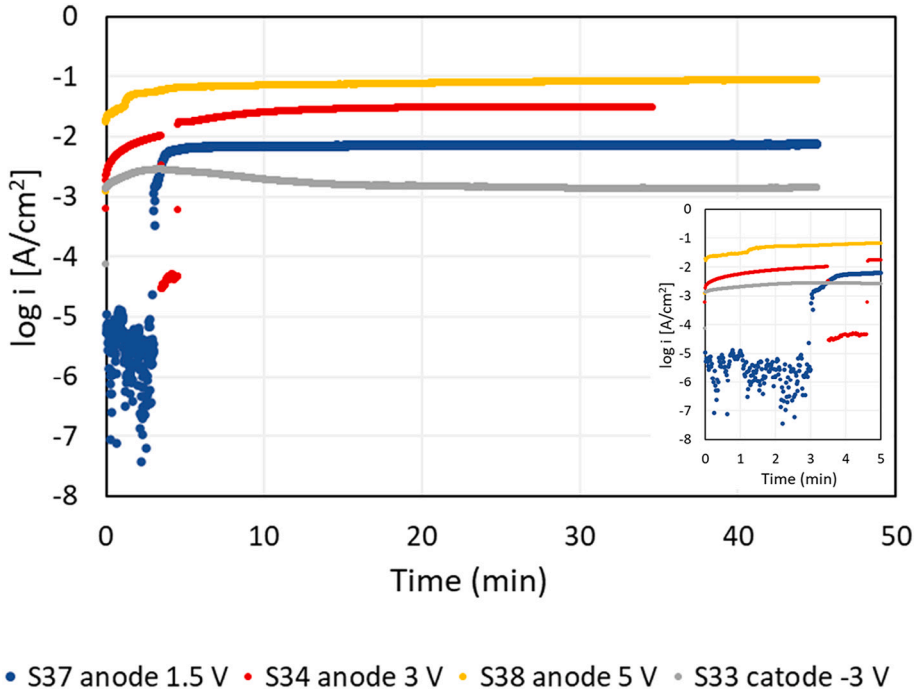

Fig. 8. Plot of log i (current/surface area) against time for SS316 samples coated with epoxy/CNF and immersed in scaling solution for 45 min. An enlarged section of the plot is shown at the bottom right, showing data from the first five minutes of the experiments.

3.7. Long term exposure at low and high polarization potentials

In order to test whether the coatings withstand longer polarization at low potentials the samples were polarized for 6 h in similar scaling solution as for the short-term exposure (45 min). Fig. 9 compares SEM images of the initial (nonpolarized) coating surface with surfaces polarized at +1.5 and + 5 V_{OCP} for 6 h.

The initial sample had a smooth and homogenous surface except for a few particles present (being most likely contamination from air, e.g., dust particles). The sample polarized at +1.5 V_{OCP} had more precipitate than the sample polarized with the same potential in shorter time (45 min in Fig. 4). No clear evidence of degradation upon polarization at +1.5 V_{OPC} after 6 h was found. Fig. 9c shows a strongly damaged surface for the sample polarized at +5 V_{OCP} for 6 h. After the sample was

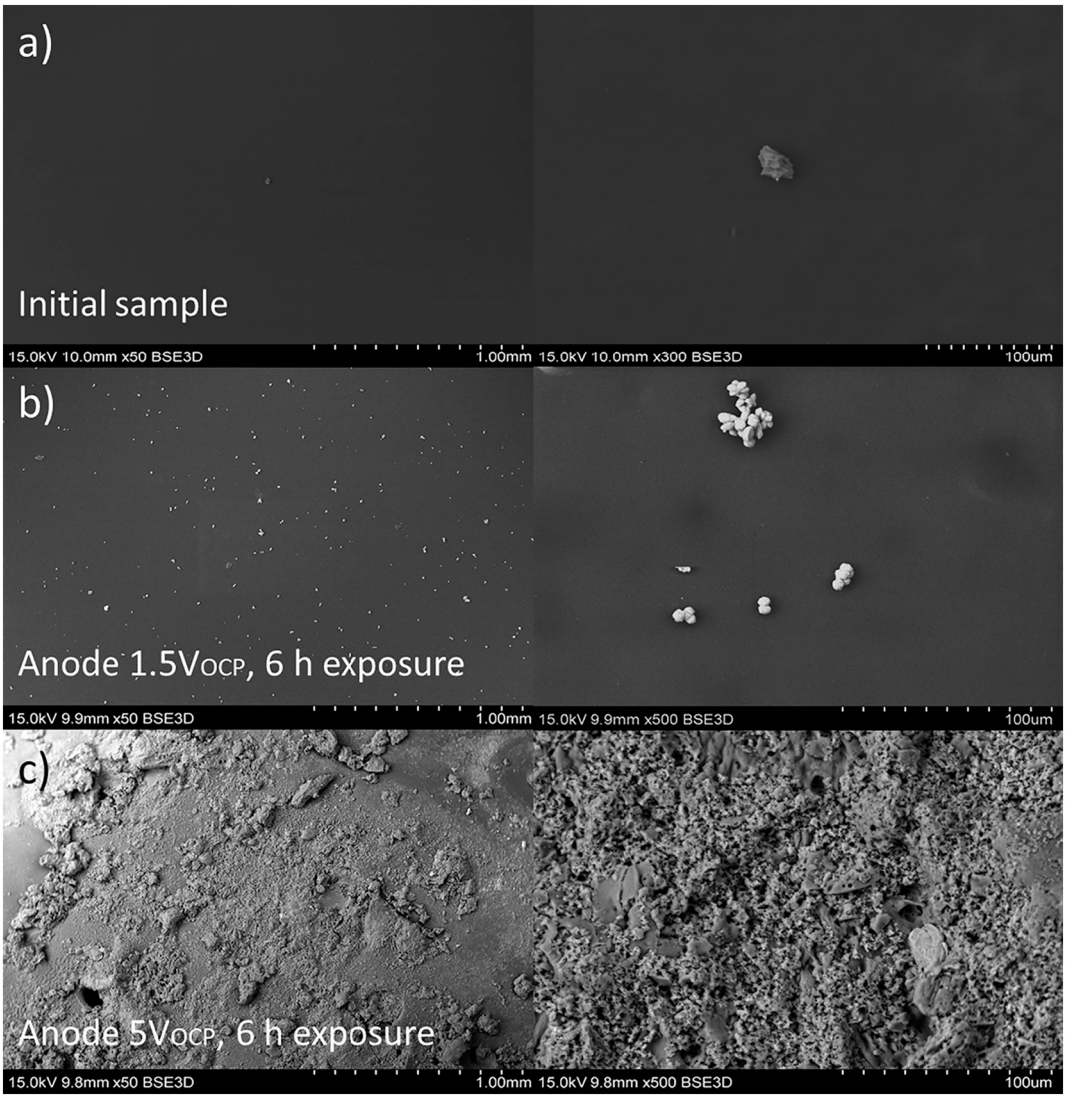

Fig. 9. SEM images presenting topography of (a) a sample surface without any exposure (initial sample), and samples subjected to polarization at potentials of (b) +1.5 V_{OCP} and (c) +5 V_{OCP} for 6 h. The enlarged image (100 μm) depicts the largest features found in the 1 mm image and are thus not representative for the whole surface.

removed from the solution, large fragments of the coating fell off. The scaling solution was also discoloured, indicating severe corrosion not only of the coating but also the underlying steel, suggesting that applying anodic polarization potential of +5 V_{OCP} was destructive for the coating and the underlying steel substrate in contrast to +1.5 V_{OCP}.

4. Conclusion

In this paper it is demonstrated, for the first time, that polarization of steel coated with epoxy/CNF composite material can be utilized to either prevent surface from scaling or enhance scaling of pH sensitive scaling minerals. Deposition of $CaCO_3$ on the epoxy/CNF surface was inhibited by anodic polarization while cathodic polarization accelerated the deposition of calcium carbonate on the coating surface. The scale acceleration and inhibition processes were driven by local changes in pH near the electrode surfaces. Polarization potential influenced the deposit of $CaCO_3$ on the cathode significantly. Anodic scale protection was found to be more pronounced at higher polarization potentials, however application of very high anodic polarization potential can be limited due to degradation of epoxy/CNF coating. Degradation of the epoxy/CNF coating increased with increasing positive potential. The degradation was most likely caused by atomic oxygen and chlorine gas evolution at the anode surface that could have contributed to the damages of carbon fibre and epoxy matrix. At lower anodic polarization potentials i.e., +1.5 and + 2 V_{OCP}, the epoxy/CNF surfaces were free from any traces of degradation and the scale deposition was significantly limited, which proves the anodic scale protection concept using conductive epoxy/CNF coatings feasible at relatively low polarization potentials. Nevertheless, long term exposure tests (longer than 6 h studied in this paper) have to be performed to reveal the lifetime of the coating under polarization.

There are several suggestions for further work this paper opens for: (i) There is a need to develop coatings that can tackle higher anodic polarization potentials without degrading or defining the conditions at which degradation is limited while surface scaling is prevented. (ii) More in depth understanding of pH development near steel surface with and without coatings has to be gained.

CRediT authorship contribution statement

Laura Edvardsen: Conceptualization, Methodology, Investigation, Writing – original draft, Writing – review & editing, Project administration. **Mathieu Grandcolas:** Conceptualization, Methodology,

Investigation, Resources, Writing – original draft, Writing – review & editing. **Sigrid Lædre:** Conceptualization, Methodology, Investigation, Resources, Writing – original draft, Writing – review & editing. **Juan Yang:** Conceptualization, Methodology, Resources, Writing – original draft. **Torstein Lange:** Conceptualization, Methodology, Resources, Writing – original draft. **Ruben Bjørge:** Investigation, Writing – original draft. **Kamila Gawel:** Conceptualization, Methodology, Resources, Writing – original draft, Writing – review & editing, Supervision, Project administration, Funding acquisition.

Declaration of competing interest

The authors declare that they have no known competing financial interests or personal relationships that could have appeared to influence the work reported in this paper.

Acknowledgements

The authors gratefully acknowledge the financial support from: (1) the strategic SINTEF Industry project number 102021203 "Electrophoretic cleaning and friction reduction for applications in drilling and well construction" and (2) The Norwegian Research Council in the form of grant number 285568 "Well fossilization for P&A". The use of the X-ray laboratory at NTNU is gratefully acknowledged.

References

[1] Y. Zhang, et al., The kinetics of carbonate scaling—application for the prediction of downhole carbonate scaling, J. Pet. Sci. Eng. 29 (2) (2001) 85–95.
[2] C. Gabrielli, et al., Study of calcium carbonate scales by electrochemical impedance spectroscopy, Electrochim. Acta 42 (8) (1997) 1207–1218.
[3] N. Andritsos, A. Karabelas, P. Koutsoukos, Scale Formation in Geothermal Plants, 2002.
[4] A. Dirany, P. Drogui, M.A. El Khakani, Clean electrochemical deposition of calcium carbonate to prevent scale formation in cooling water systems, Environ. Chem. Lett. 14 (4) (2016) 507–514.
[5] H.-J. Lee, et al., A comparative study of RO membrane scale inhibitors in wastewater reclamation: antiscalants versus pH adjustment, Sep. Purif. Technol. 240 (2020), 116549.
[6] M.K. Shahid, M. Pyo, Y.-G. Choi, Carbonate scale reduction in reverse osmosis membrane by CO2 in wastewater reclamation, Membr. Water Treat. 8 (2) (2017) 125–136.
[7] J. MacAdam, S.A. Parsons, Calcium carbonate scale formation and control, Rev. Environ. Sci. Biotechnol. 3 (2) (2004) 159–169.
[8] P.W. Hart, G.W. Colson, J. Burris, Application of carbon dioxide to reduce water-side lime scale in heat exchangers, J. Sci. Technol. For. Prod. Process 1 (2011) 67–70.
[9] L. Edvardsen, et al., Electrochemical enhancement and inhibition of calcium carbonate deposition, J. Environ. Chem. Eng. 8 (5) (2020), 104239.
[10] B. Pečnik, et al., Scale deposit removal by means of ultrasonic cavitation, Wear 356 (2016) 45–52.
[11] U. Sahin, T. Tunc, S. Eroğlu, Evaluation of CaCO3 clogging in emitters with magnetized saline waters, Desalin. Water Treat. 40 (1–3) (2012) 168–173.
[12] M. Gryta, The influence of magnetic water treatment on CaCO3 scale formation in membrane distillation process, Sep. Purif. Technol. 80 (2) (2011) 293–299.
[13] J. Coey, S. Cass, Magnetic water treatment, J. Magn. Magn. Mater. 209 (1–3) (2000) 71–74.
[14] T. Okazaki, et al., Investigation of the effects of electromagnetic field treatment of hot spring water for scale inhibition using a fibre optic sensor, Sci. Rep. 9 (1) (2019) 1–8.
[15] L. Lin, et al., A critical review of the application of electromagnetic fields for scaling control in water systems: mechanisms, characterization, and operation, npj Clean Water 3 (1) (2020) 1–19.
[16] J.E. Friis, et al., Evaluation of surface-initiated polymer brush as anti-scaling coating for plate heat exchangers, Prog. Org. Coat. 136 (2019), 105196.
[17] J. Zhao, et al., A review of heterogeneous nucleation of calcium carbonate and control strategies for scale formation in multi-stage flash (MSF) desalination plants, Desalination 442 (2018) 75–88.
[18] A. Persat, M.E. Suss, J.G. Santiago, Basic principles of electrolyte chemistry for microfluidic electrokinetics. Part II: coupling between ion mobility, electrolysis, and acid–base equilibria, Lab Chip 9 (17) (2009) 2454–2469.
[19] K. Sheng, et al., Formation and inhibition of calcium carbonate crystals under cathodic polarization conditions, Crystals 10 (4) (2020) 275.
[20] R.Y. Khaled, A. Abdel-Gaber, A comparative study of corrosion inhibition of steel and stainless steel in hydrochloric acid by N, N, N′, N′-tetramethyl-p-phenylenediamine, Prot. Met. Phys. Chem. Surf. 53 (5) (2017) 956–960.
[21] P. Cardoso, et al., The dominant role of tunneling in the conductivity of carbon nanofiber-epoxy composites, Phys. Status Solidi A 207 (2) (2010) 407–410.
[22] A. Allaoui, S.V. Hoa, M.D. Pugh, The electronic transport properties and microstructure of carbon nanofiber/epoxy composites, Compos. Sci. Technol. 68 (2) (2008) 410–416.
[23] P. Cardoso, et al., The influence of the dispersion method on the electrical properties of vapor-grown carbon nanofiber/epoxy composites, Nanoscale Res. Lett. 6 (1) (2011) 1–5.
[24] L. Guadagno, et al., The role of carbon nanofiber defects on the electrical and mechanical properties of CNF-based resins, Nanotechnology 24 (30) (2013), 305704.
[25] F. Marra, et al., Electromagnetic and dynamic mechanical properties of epoxy and vinylester-based composites filled with graphene nanoplatelets, Polymers 8 (8) (2016) 272.
[26] S. Rana, R. Alagirusamy, M. Joshi, Development of carbon nanofibre incorporated three phase carbon/epoxy composites with enhanced mechanical, electrical and thermal properties, Compos. A: Appl. Sci. Manuf. 42 (5) (2011) 439–445.
[27] L.-H. Sun, et al., Preparation, characterization, and modeling of carbon nanofiber/epoxy nanocomposites, J. Nanomater. 2011 (2011).
[28] S. Wu, et al., Epoxy nanocomposites containing magnetite-carbon nanofibers aligned using a weak magnetic field, Polymer 68 (2015) 25–34.
[29] I. Aziz, et al., The role of interface on dynamic mechanical properties, dielectric performance, conductivity, and thermal stability of electrospun carbon nanofibers reinforced epoxy, Polym. Compos. (2021).
[30] W. Duan, et al., Electrochemical mineral scale prevention and removal on electrically conducting carbon nanotube–polyamide reverse osmosis membranes, Environ Sci Process Impacts 16 (6) (2014) 1300–1308.
[31] J. Czyżewski, et al., Rapid prototyping of electrically conductive components using 3D printing technology, J. Mater. Process. Technol. 209 (12) (2009) 5281–5285.
[32] J.-M. Park, et al., Self-sensing of carbon fiber/carbon nanofiber–epoxy composites with two different nanofiber aspect ratios investigated by electrical resistance and wettability measurements, Compos. A: Appl. Sci. Manuf. 41 (11) (2010) 1702–1711.
[33] K.-Y. Law, Definitions for Hydrophilicity, Hydrophobicity, and Superhydrophobicity: Getting the Basics Right, ACS Publications, 2014.
[34] C. Compere, N. Lebozec, Behaviour of Stainless Steel in Natural Seawater, 1997.
[35] Q. Liang, G. Brocks, A. Bieberle-Hütter, Oxygen evolution reaction (OER) mechanism under alkaline and acidic conditions, J. Phys. Energy 3 (2) (2021), 026001.
[36] M. Favaro, et al., Elucidating the alkaline oxygen evolution reaction mechanism on platinum, J. Mater. Chem. A 5 (23) (2017) 11634–11643.
[37] G.R. Stafford, G.L. Cahen Jr., G.E. Stoner, Graphite fiber-polymer matrix composites as electrolysis electrodes, J. Electrochem. Soc. 138 (2) (1991) 425.
[38] R. Beck, J.-P. Andreassen, Spherulitic growth of calcium carbonate, Cryst. Growth Des. 10 (7) (2010) 2934–2947.
[39] S.U. Ofoegbu, M.G. Ferreira, M.L. Zheludkevich, Galvanically stimulated degradation of carbon-fiber reinforced polymer composites: a critical review, Materials 12 (4) (2019) 651.
[40] F. Sloan, J. Talbot, Corrosion of graphite-Fiber-reinforced composites IIAnodic polarization damage, Corrosion 48 (12) (1992).
[41] S. Agrawal, et al., Effect of aqueous HCl with dissolved chlorine on certain corrosion-resistant polymers, ACS Omega 3 (6) (2018) 6692–6702.
[42] S. Taylor, F. Wall, G. Cahen jr., The detection and analysis of electrochemical damage in bismaleimide/graphite fiber composites, J. Electrochem. Soc. 143 (2) (1996) 449.
[43] A. Currao, Photoelectrochemical water splitting, CHIMIA Int. J. Chem. 61 (12) (2007) 815–819.